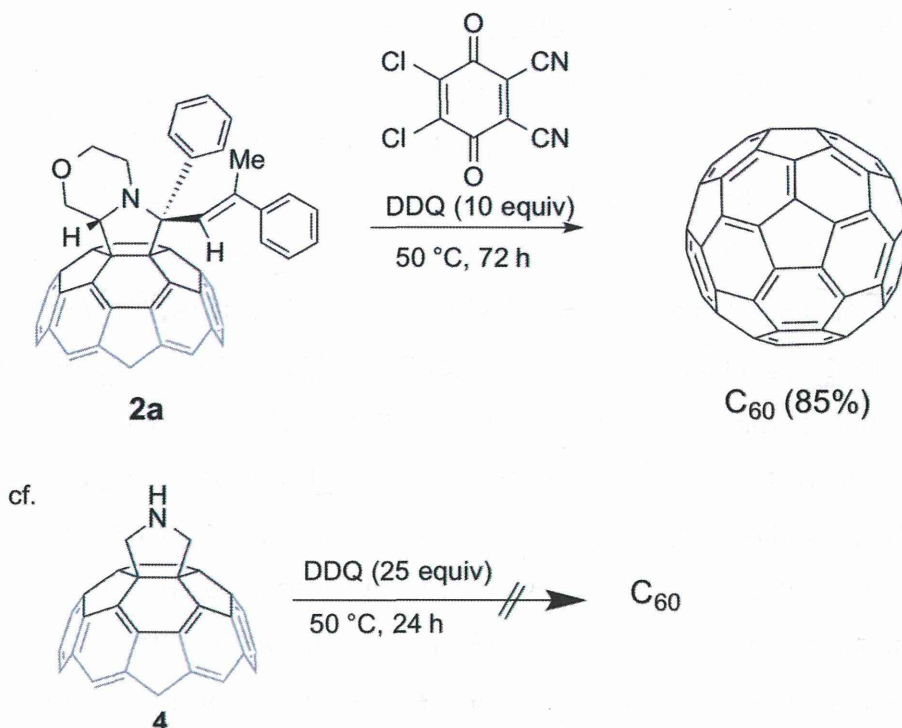pyrrolidinofullerene **4**[1] was not oxidized by DDQ, the oxidative abstraction of methine proton of pyrrolidine ring of **2a** seems to be essential for the cycloreversion.

Scheme 3

EXPERIMENTAL

General Synthetic Procedure of 2: The solution of cyclic amines (100 mmol), arylketone (100 mmol), and catalytic amount of *p*-toluenesulfonic acid (TsOH, <100 mg) in toluene (50 mL) was stirred at refluxing temperature (140 °C) under nitrogen for 5–10 h using a Dean-Stark apparatus. After the removal of solvent, unreacted acetophenone and morpholine were almost removed in vacuo. The residue was diluted with pentane to precipitate TsOH, then filtrated and evaporated. Crude products **1b–h** were employed in the next reaction without further purifications. The solution of C_{60} (100 mg, 0.14 mmol) and dienamines **1** (ca. 3.5 mmol, 25 equiv) in toluene (50 mL) was stirred in dark at 90 °C under nitrogen. The reaction was traced by HPLC (Buckyprep, toluene eluent). After filtration, the solvent was removed in vacuo. The residue was chromatographed on silica gel to provide the monoadduct **2b–h**.

Compound 2b. ^{1}H-NMR: (600 MHz, CDCl$_3$) δ 1.80 (s, 3H), 2.01–2.09 (m, 2H), 2.17–2.23 (m, 2H), 2.31–2.34 (dd, 1H, *J* = 6.8, 13.4 Hz), 2.71–2.74 (m, 2H), 3.61–3.63 (d, 1H, *J* = 10.9 Hz), 4.59–4.61 (dd, 1H, *J* = 3.0, 11.2 Hz), 7.25–7.27 (m, 2H), 7.30–7.33 (t, 1H, *J* = 7.5 Hz), 7.38–7.41 (t, 2H, *J* = 7.9 Hz), 7.45–7.48 (m, 1H), 7.46 (s, 1H), 7.59–7.61 (d, 2H, *J* = 7.3 Hz), 7.71–7.73 (d, 1H, *J* = 6.9 Hz), 8.23–8.24 (d, 1H, *J* = 8.0 Hz). ^{13}C-NMR: (150 MHz, CDCl$_3$) δ 20.73, 25.26, 25.88, 32.33, 47.77, 69.99, 73.41, 79.71, 81.97, 126.39, 127.41, 127.72, 127.75, 127.80, 128.25, 128.69, 128.86, 130.28, 135.81, 136.03, 136.53, 137.49, 138.51, 139.42, 139.49, 139.96, 140.25, 141.24, 141.60, 141.65, 141.75, 141.78, 141.93,

141.99, 142.08, 142.12, 142.15, 142.30, 142.33, 142.46, 142.53, 142.66, 142.69, 143.05, 143.15, 143.24, 144.35, 144.41, 144.62, 144.66, 144.83, 145.08, 145.12, 145.14, 145.16, 145.21, 145.23, 145.27, 145.52, 145.59, 145.60, 145.79, 145.80, 145.84, 146.10, 146.12, 146.15, 146.21, 146.32, 146.36, 146.92, 146.99, 147.25, 147.29, 147.35, 152.82, 154.50, 154.62, 155.79. MS (MALDI-MS): m/z = 1009.

Compound 2c. ^{1}H-NMR: (600 MHz, CDCl$_3$) δ 1.81 (s, 3H), 3.05–3.10 (dt, 1H, J = 3.5, 11.4 Hz), 3.40–3.42 (d, 1H, J = 11.0 Hz), 4.10–4.14 (dt, 1H, J = 2.6, 11.4 Hz), 4.22–4.26 (t, 1H, J = 10.3 Hz), 4.24–4.26 (d, 1H, J = 10.5 Hz), 4.75–4.77 (dd, 1H, J = 3.2, 10.1 Hz), 4.81–4.83 (dd, 1H, J = 3.1, 10.5 Hz), 7.30–7.32 (dd, 1H, J = 2.3, 8.5 Hz), 7.41–7.43 (m, 1H), 7.42–7.43 (d, 1H, J = 8.7 Hz), 7.44 (s, 1H), 7.48–7.50 (dd, 1H, J = 2.3, 8.5 Hz), 7.55–7.57 (m, 1H), 7.55–7.57 (d, 1H, J = 8.7 Hz), 7.66–7.68 (dd, 1H, J = 2.3, 8.5 Hz), 8.19–8.21 (dd, 1H, J = 2.3, 8.5 Hz) ^{13}C-NMR: (150 MHz, CDCl$_3$) δ 20.74, 47.86, 66.74, 67.48, 70.87, 71.82, 79.06, 82.13, 126.79, 127.59, 128.76, 128.85, 129.07, 131.23, 133.80, 133.81, 135.80, 136.12, 136.54, 137.36, 138.06, 138.92, 139.49, 139.75, 140.35, 141.33, 141.54, 141.60, 141.65, 141.80, 141.94, 141.96, 142.03, 142.09, 142.23, 142.29, 142.30, 142.33, 142.47, 142.59, 142.71, 142.74, 143.09, 143.28, 144.30, 144.33, 144.47, 144.53, 144.71, 145.16, 145.19, 145.22, 145.24, 145.28, 145.33, 145.34, 145.42, 145.60, 145.68, 145.87, 145.93, 146.15, 146.16, 146.19, 146.28, 146.34, 146.38, 146.48, 146.58, 147.30, 147.38, 152.07, 152.94, 153.31, 153.37. MS (MALDI-MS): m/z = 1079.

Compound 2d. ^{1}H-NMR: (600 MHz, CDCl$_3$) δ 1.81 (s, 3H), 2.34 (s, 3H), 2.41 (s, 3H), 3.07–3.11 (dt, 1H, J = 3.4, 11.4 Hz), 3.45–3.47 (d, 1H, J = 10.9 Hz), 4.10–4.14 (dt, 1H, J = 2.8, 11.4 Hz), 4.22–4.24 (d, 1H, J = 11.1 Hz), 4.22–4.26 (d, 1H, J = 10.9 Hz), 4.79–4.81 (t, 1H, J = 7.9 Hz), 4.79–4.82 (t, 1H, J = 7.6 Hz), 7.10–7.11 (d, 1H, J = 8.1 Hz), 7.26–7.29 (m, 2H), 7.46 (s, 1H), 7.54–7.56 (d, 2H, J = 8.2 Hz), 7.59–7.61 (dd, 1H, J = 1.9, 8.1 Hz), 8.10–8.12 (dd, 1H, J = 1.9, 8.1 Hz). ^{13}C-NMR: (150 MHz, CDCl$_3$) δ 20.70, 21.15, 21.25, 47.84, 66.89, 67.35, 71.00, 71.90, 79.50, 82.54, 126.04, 126.18, 127.43, 129.27, 129.32, 129.37, 130.13, 135.57, 136.30, 136.43, 136.82, 137.34, 137.43, 137.60, 138.70, 139.35, 139.60, 140.24, 141.30, 141.49, 141.61, 141.66, 141.71, 141.92, 141.97, 142.00, 142.09, 142.25, 142.27, 142.32, 142.40, 142.53, 142.63, 142.64, 142.66, 143.02, 143.09, 143.22, 144.30, 144.36, 144.57, 144.62, 144.68, 145.08, 145.10, 145.13, 145.8, 145.21, 145.25, 145.26, 145.49, 145.64, 145.68, 145.81, 145.87, 146.07, 146.10, 146.21, 146.30, 146.35, 146.80, 147.05, 147.27, 152.81, 153.70, 153.84, 153.93. MS (MALDI-MS): m/z = 1039.

Compound 2e. ^{1}H-NMR: (600 MHz, CDCl$_3$) δ 1.19–1.21 (t, 3H, J = 7.6 Hz), 1.28–1.30 (t, 3H, J = 7.6 Hz), 1.813 (s, 3H), 2.61–2.65 (q, 2H, J = 7.6 Hz), 2.69–2.73 (q, 2H, J = 7.6 Hz), 3.08–3.12 (dt, 1H, J = 3.5, 11.4 Hz), 3.47–3.49 (d, 1H, J = 11.0 Hz), 4.10–4.15 (dt, 1H, J = 2.3, 11.4 Hz), 4.23–4.26 (t, 1H, J = 11.0 Hz), 4.22–4.24 (d, 1H, J = 11.1 Hz), 4.80–4.81 (d, 1H, J = 10.5 Hz), 4.80–4.81 (d, 1H, J = 10.3 Hz), 7.10–7.11 (dd, 1H, J = 1.7, 8.1 Hz), 7.29–7.31 (m, 3H), 7.49 (s, 1H), 7.58–7.60 (m, 2H), 7.61–7.62 (dd, 1H, J = 2.0, 8.1 Hz), 8.13–8.14 (dd, 1H, J = 1.9, 8.1 Hz). ^{13}C-NMR: (150 MHz, CDCl$_3$) δ 15.53, 15.60,

20.66, 28.47, 28.54, 47.82, 66.89, 67.34, 71.01, 71.89, 79.55, 82.58, 125.99, 126.22, 127.51, 128.00, 128.03, 128.14, 128.23, 129.04, 130.16, 135.50, 136.31, 136.31, 136.64, 136.84, 137.35, 138.61, 139.22, 139.34, 139.59, 140.23, 141.29, 141.59, 141.62, 141.65, 141.67, 141.71, 141.92, 141.97, 142.00, 142.09, 142.25, 142.26, 142.32, 142.52, 142.62, 142.63, 142.66, 143.02, 143.22, 143.91, 143.98, 144.30, 144.37, 144.59, 144.63, 144.67, 145.07, 145.10, 145.13, 145.14, 145.21, 145.24, 145.25, 145.49, 145.63, 145.68, 145.81, 145.86, 146.06, 146.09, 146.10, 146.19, 146.30, 146.35, 146.80, 146.84, 147.05, 147.27, 147.31, 152.81, 153.71, 153.85, 153.95. MS (MALDI-MS): m/z = 1067.

Compound 2f. ^{1}H-NMR: (600 MHz, CDCl$_3$) δ 0.82–0.84 (t, 3H, J = 7.1 Hz), 0.88–0.91 (t, 3H, J = 7.2 Hz), 1.18–1.39 (m, 16H), 1.84 (s, 3H), 2.57–2.60 (t, 2H, J = 7.4 Hz), 2.64–2.67 (t, 2H, J = 7.8 Hz), 3.09–3.13 (dt, 1H, J = 3.5, 11.4 Hz), 3.48–3.49 (d, 1H, J = 11.1 Hz), 4.10–4.14 (dt, 1H, J = 2.3, 11.4 Hz), 4.22–4.24 (d, 1H, J = 11.1 Hz), 4.22–4.26 (t, 1H), 4.80–4.81 (d, 1H, J = 10.6 Hz), 4.80–4.82 (d, 1H, J = 10.7 Hz), 7.08–7.09 (dd, 1H, J = 1.5, 8.1 Hz), 7.26–7.27 (m, 1H), 7.46–7.48 (t, 1H, J = 7.3 Hz), 7.50 (s, 1H), 7.56–7.59 (d, 2H, J = 8.4 Hz), 7.60–7.62 (dd, 1H, J = 1.8, 8.1 Hz), 7.96–7.98 (m, 1H), 8.12–8.14 (dd, 1H, J = 1.9, 8.1 Hz). ^{13}C-NMR: (150 MHz, CDCl$_3$) δ 14.15, 20.61, 22.63, 22.67, 28.54, 29.08, 31.16, 31.47, 31.71, 31.75, 35.45, 35.64, 47.80, 66.90, 67.36, 71.00, 71.89, 79.59, 82.63, 125.86, 126.12, 127.44, 128.32, 128.58, 128.66, 133.11, 135.45, 136.32, 136.72, 136.85, 137.13, 137.37, 138.56, 139.34, 139.58, 140.24, 141.29, 141.50, 141.59, 141.63, 141.69, 141.93, 141.98, 142.00, 142.09, 142.26, 142.31, 142.53, 142.62, 142.64, 142.66, 142.73, 143.02, 143.23, 144.31, 144.37, 144.60, 144.65, 144.67, 145.07, 145.11, 145.12, 145.15, 145.22, 145.25, 145.50, 145.64, 115.69, 145.82, 145.86, 146.06, 146.10, 146.11, 146.20, 146.31, 146.35, 146.81, 146.87, 147.05, 147.27, 147.32, 152.80, 153.71, 153.86, 153.95. MS (MALDI-MS): m/z = 1179.

Compound 2g. ^{1}H-NMR: (600 MHz, CDCl$_3$) δ 1.93 (s, 3H), 3.15–3.19 (dt, 1H, J = 3.3, 11.2 Hz), 3.54–3.56 (d, 1H, J = 11.0 Hz), 4.15–4.19 (dt, 1H, J = 2.4, 11.4 Hz), 4.26–4.30 (t, 1H, J = 11.6 Hz), 4.27–4.29 (d, 1H, J = 11.5 Hz), 4.83 –4.87 (t, 1H, J = 11.4 Hz), 4.84 –4.87 (t, 1H, J = 8.9 Hz), 7.32–7.35 (t, 1H, J = 7.4 Hz), 7.36–7.39 (dt, 1H, J = 7.4 Hz), 7.42–7.44 (t, 2H, J = 7.5 Hz), 7.46–7.48 (t, 2H, J = 7.5 Hz), 7.58–7.60 (dd, 1H, J = 1.9, 8.2 Hz), 7.61 (s, 1H), 7.63–7.64 (dd, 2H, J = 1.2, 8.4 Hz), 7.66–7.67 (dd, 1H, J = 1.2, 8.4 Hz), 7.70–7.71 (m, 2H), 7.75–7.78 (m, 3H), 7.82–7.84 (dd, 1H, J = 1.9, 8.2 Hz), 8.33–8.34 (dd, 1H, J = 1.9, 8.2 Hz). ^{13}C-NMR: (150 MHz, CDCl$_3$) δ 20.75, 47.96, 66.90, 67.49, 71.05, 71.92, 79.53, 82.51, 126.71, 126.98, 127.06, 127.23, 127.38, 127.45, 128.08, 128.82, 128.86, 130.59, 135.69, 136.29, 136.77, 137.43, 138.65, 138.76, 139.43, 139.67, 140.31, 140.34, 140.38, 140.55, 140.71, 141.31, 141.64, 141.67, 141.78, 141.95, 141.99, 142.03, 142.10, 142.25, 142.28, 142.35, 142.55, 142.66, 142.67, 142.70, 143.04, 143.06, 143.10, 143.25, 144.33, 144.37, 144.57, 144.60, 144.69, 145.12, 145.17, 145.19, 145.23, 145.27, 145.30, 145.50, 145.67, 145.84, 145.89, 146.11, 146.13, 146.16, 146.23, 146.34,

146.38, 146.72, 146.75, 146.90, 147.29, 147.34, 152.59, 153.56, 153.64, 153.66. MS (MALDI-MS): m/z = 1163.

Compound 2h. ^{1}H-NMR: (600 MHz, CDCl$_3$) δ 2.06 (s, 3H), 3.13–3.17 (dt, 1H, J = 3.3, 11.1 Hz), 3.79 (br, 1H), 4.09–4.13 (dt, 1H, J =2.1, 11.6 Hz), 4.20–4.23 (m, 2H), 4.70-4.73 (dd, 1H, J = 3.1, 10.1 Hz), 4.78–4.80 (dd, 1H, J =3.3, 10.6 Hz), 7.01 (br, 1H), 7.08–7.10 (dd, 2H, J = 3.5, 5.0 Hz), 7.23–7.24 (dd, 1H, J = 1.1, 3.6 Hz), 7.27–7.28 (d, 1H, J = 4.9 Hz), 7.33 (br, 1H), 7.75 (s, 1H). ^{13}C-NMR: (150 MHz, CDCl$_3$) δ 20.11, 29.68, 66.74, 70.66, 71.56, 76.57, 82.99, 123.98, 124.86, 127.80, 136.35, 136.55, 137.26, 138.70, 139.62, 140.25, 141.31, 141.41, 141.55, 141.59, 141.77, 141.93, 142.03, 142.13, 142.26, 142.39, 142.55, 142.60, 142.68, 143.05, 143.23, 144.30, 144.36, 144.46, 144.56, 144.69, 145.07, 145.14, 145.24, 145.33, 145.53, 145.67, 145.83, 145.87, 146.04, 146.08, 146.13, 146.26, 146.33, 146.39, 146.57, 147.29, 147.35, 147.79, 153.19, 153.47. MS (MALDI-MS): m/z = 1024 ([M+H]).

Compound 3a by TfOH acidification. To the solution of **2a** (5 mg, 0.0049 mmol) in chlorobenzene, trifluoromethanesulfonic acid (TfOH, 18 mg, 0.12 mmol) was dropwisely added. The solution was stirred 5 h at 80 °C. The reaction was quenched by adding water, and extracted with chlorobenzene. The solution was concentrated in vacuo. The product was purified by column chromatography, to give **3a** (3.30 mg, 59%). ^{1}H-NMR: (600 MHz, CDCl$_3$) δ 1.93 (s, 3H), 2.82–2.83 (d, 1H, J = 10.3 Hz), 3.08–3.12 (dt, 1H, J = 4.9, 11.2 Hz), 3.38–3.41 (d, 1H, J = 14.7 Hz), 3.97–4.01 (dt, 1H, J = 2.5, 11.2 Hz), 3.98–4.01 (d, 1H, J = 14.7 Hz), 4.20–4.22 (d, 1H, , J = 10.6 Hz), 4.21–4.24 (t, 1H, J = 10.6 Hz), 4.43–4.45 (dd, 1H, J = 3.4, 10.3 Hz), 4.81–4.83 (dd, 1H, J = 3.4, 10.6 Hz), 6.99–7.02 (t, 1H, J = 7.3 Hz), 7.04–7.07 (t, 2H, J = 7.8 Hz), 7.19–7.21 (d, 2H, J = 7.2 Hz), 7.42–7.45 (dt, 1H, J = 1.2, 7.7 Hz), 7.46–7.47 (d, 1H, J = 7.7 Hz), 7.51–7.54 (dt, 1H, J = 1.2, 7.7 Hz), 7.85–7.87 (d, 1H, J = 7.7 Hz). ^{13}C-NMR: (150 MHz, CDCl$_3$) δ 33.77, 44.88, 45.52, 51.08, 67.06, 71.39, 71.96, 80.26, 85.07, 126.08, 127.03, 127.23, 128.23, 128.75, 129.36, 136.38, 136.59, 136.75, 139.10, 139.53, 139.76, 139.99, 140.63, 141.32, 141.37, 141.47, 141.69, 141.81, 141.86, 141.98, 141.99, 142.05, 142.14, 142.38, 142.54, 142.58, 142.76, 143.14, 144.00, 144.22, 144.50, 144.58, 144.85, 145.08, 145.12, 145.16, 145.22, 145.28, 145.30, 145.52, 145.56, 145.82, 145.88, 145.93, 146.00, 146.15, 146.21, 146.26, 146.61, 146.80, 147.15, 147.2, 148.82, 150.65, 153.48, 153.75, 153.93, 154.43.

Oxidation of pyrrolidinofullerene 2a. DDQ (22.4 mg, 0.10 mmol) was added in the chlorobenzene solution of **2a** (10.0 mg, 0.098 mmol). The mixture was slightly warmed at 50 °C with stirring 72 h. After cooling to rt, water and chlorobenzene were added to the solution. The organic layer was separated and evapolated. The residue was purified by column chromatography, to give pristine C$_{60}$ (6.1 mg, 85%).

ACKNOWLEDGEMENTS

REFERENCES AND NOTES

1. a) M. Maggini, G. Scorrano, and M. Prato, *J. Am. Chem. Soc.*, 1993, **115**, 9798; b) M. Prato and M. Maggini, *Acc. Chem. Res.*, 1998, **31**, 519.

2. Y. Zhao, L. Gan, D. Zhou, C. Luo, and C. Huang, *Chin. Sci. Bull.*, 1997, **42**, 1360.

3. A. Bianco, M. Maggini, and G. Scorrano, *J. Am. Chem. Soc.*, 1996, **118**, 4072.

4. S. Filippone, E. E. Maroto, A. Martín-Domenech, M. Suárez, and N. Martín, *Nature Chem.*, 2009, **1**, 578.

5. a) S. Campidelli, R. Deschenaux, J.-F. Eckert, D. Guillon, and J.-F. Nierengarten, *Chem. Commun.*, 2002, 656; J. Lenoble, N. Maringa, S. Campidelli, B. Donnio, D. Guillon, and R. Deschenaux, *Org. Lett.*, 2006, **8**, 1851.

6. a) H. Imahori, K. Hagiwara, T. Akiyama, M. Aoki, S. Taniguchi, T. Okada, M. Shirakawa, and Y. Sakata, *Chem. Phys. Lett.*, 1996, **263**, 545; b) P. A. Troshin, A. S. Peregudov, S. I. Troyanov, and R. N. Lyubovskaya, *Russ. Chem. Bull.*, 2009, **57**, 887.

7. N. Ikuma, H. Yamamoto, K. Kokubo, and T. Oshima, *Chem. Lett.*, 2014, **43**, 1648.

8. R. S. Ashraf, M. Shahid, E. Klemm, M. Al-Ibrahim, and S. Sensfuss, *Macromol. Rapid Commun.*, 2006, **27**, 1454.

9. T. Michinobu, T. Nakanishi, J. P. Hill, M. Funahashi, and K. Ariga, *J. Am. Chem. Soc.*, 2006, **128**, 10384.

10. MALDI-MS of **2a** showed the fragment peak due to the elimination of methylstyrene (M–117) as shown in ref. 7.

11. K. Kokubo, S. Tochika, M. Kato, Y. Sol, and T. Oshima, *Org. Lett.*, 2008, **10**, 3335.

12. a) G. A. Olah, I. Bucsi, and C. Lambert, *J. Am. Chem. Soc.*, 1991, **113**, 9388; b) A. Iwashita, Y. Matsuo, and E. Nakamura, *Angew. Chem. Int. Ed.*, 2007, **46**, 3513.

13. Although pristine fullerene was inactive with TfOH, fullerene derivatives having basic sites reacted with TfOH, followed by arylation of aromatic solvents. See: M. Nambo, Y. Segawa, and K. Itami, *J. Am. Chem. Soc.*, 2011, **133**, 2402.

14. a) N. Martín, M. Altable, S. Filippone, A. Martín-Domenech, L. Echegoyen, and C. M. Cardona, *Angew. Chem. Int. Ed.*, 2006, **45**, 110; b) S. Filippone, M. I. Barroso, A. Martín-Domenech, S. Osuna, M. Solà, and N. Martín, *Chem. Eur. J.*, 2008, **14**, 5198.

Pyrrolidinium fullerene induces apoptosis by activation of procaspase-9 *via* suppression of Akt in primary effusion lymphoma

CrossMark

Tadashi Watanabe [a], Shigeo Nakamura [b], Toshiya Ono [c], Sadaharu Ui [c], Syota Yagi [a], Hiroki Kagawa [a], Hisami Watanabe [d], Tomoyuki Ohe [e], Tadahiko Mashino [e], Masahiro Fujimuro [a,*]

[a] *Department of Cell Biology, Kyoto Pharmaceutical University, Misasagi-Shichonocho 1, Yamashinaku, Kyoto 607-8412, Japan*
[b] *Department of Chemistry, Nippon Medical School, 1-7-1 Kyonan-cho, Musashino, Tokyo 180-0023, Japan*
[c] *Department of Biotechnology, Interdisciplinary Graduate School of Medicine and Engineering, University of Yamanashi, Kofu 400-8511, Japan*
[d] *Center of Molecular Biosciences, Tropical Biosphere Research Center, University of the Ryukyus, 1 Senbaru, Nishihara-cho, Okinawa 903-0213, Japan*
[e] *Department of Pharmaceutical Sciences, Faculty of Pharmacy, Keio University, 1-5-30 Shibakoen, Minato-ku, Tokyo 105-8512, Japan*

ARTICLE INFO

ABSTRACT

Primary effusion lymphoma (PEL) is a subtype of non-Hodgkin's B-cell lymphoma and is an aggressive neoplasm caused by Kaposi's sarcoma-associated herpesvirus (KSHV) in immunosuppressed patients. In general, PEL cells are derived from post-germinal center B-cells and are infected with KSHV. To evaluate potential novel anti-tumor compounds against KSHV-associated PEL, seven water-soluble fullerene derivatives were evaluated as potential drug candidates for the treatment of PEL. Herein, we discovered a pyrrolidinium fullerene derivative, 1,1,1′,1′-tetramethyl [60]fullerenodipyrrolidinium diiodide, which induced apoptosis of PEL cells *via* a novel mechanism, the caspase-9 activation by suppressing the caspase-9 phosphorylation, causing caspase-9 inactivation. Pyrrolidinium fullerene treatment reduced significantly the viability of PEL cells compared with KSHV-uninfected lymphoma cells, and induced the apoptosis of PEL cells by activating caspase-9 *via* procaspase-9 cleavage. Pyrrolidinium fullerene additionally reduced the Ser473 phosphorylation of Akt and Ser196 of procaspase-9. Ser473-phosphorylated Akt (i.e., activated Akt) phosphorylates Ser196 in procaspase-9, causing inactivation of procaspase-9. We also demonstrated that Akt inhibitors suppressed the proliferation of PEL cells compared with KSHV-uninfected cells. Our data therefore suggest that Akt activation is essential for cell survival in PEL and a pyrrolidinium fullerene derivative induced apoptosis by activating caspase-9 *via* suppression of Akt in PEL cells. In addition, we evaluated whether pyrrolidinium fullerene in combination with the HSP90 inhibitor (geldanamycin; GA) or valproate, potentiated the cytotoxic effects on PEL cells. Compared to treatment with pyrrolidinium fullerene alone, the addition of low-concentration GA or valproate enhanced the cytotoxic activity of pyrrolidinium fullerene. These results indicate that pyrrolidinium fullerene could be used as a novel therapy for the treatment of PEL.

© 2014 Elsevier Inc. All rights reserved.

1. Introduction

Primary effusion lymphoma (PEL; also called body cavity-based lymphoma) is classified as a non-Hodgkin's B-cell lymphoma developing in immunocompromised patients, such as acquired immunodeficiency syndrome (AIDS) patients or those who have undergone organ transplantation [1,2]. PEL cells are infected with KSHV (also known as human herpesvirus-8) and often with EBV.

KSHV is the causative herpesvirus of Kaposi's sarcoma, PEL and multicentric Castleman's disease [3]. During a latent infection, the KSHV genome circularizes to form a double-stranded episome in the nucleus of PEL cells. KSHV establishes a latent infection in PEL cells and expresses several viral molecules, including LANA, vFLIP, vIRF3 and microRNAs. These molecules dysregulate p53, Wnt, NF-κB, Akt, Erk and interferon signaling to maintain the malignant phenotype and to ensure PEL cell survival, proliferation and immune escape [4–6]. Specifically, KSHV activates Akt signaling, allowing the survival of infected cells and the protection of infected cells from apoptosis [7]. PI3K-PDK1 and mTOR complex2 (mTORC2) induce Akt phosphorylation leading to Akt activation, which facilitates cell survival and anti-apoptosis by inhibiting

GSK-3β, forkhead transcription factors (FoxO), Bad and procaspase-9 [8]. In particular, activated Akt, (Akt phosphorylated at Ser473) can phosphorylate Ser196 of procaspase-9, resulting in suppression of procaspase-9 activation by proteolytic cleavage of procaspase-9 [9,10]. Regarding the cascade of caspase-9-mediated apoptosis, apoptotic stimuli—including DNA damage and mitochondrial disorder—induce the release of cytochrome c from mitochondria into the cytosol, where cytochrome c interacts with Apaf-1, inducing binding to procaspase-9, resulting in proteolytic cleavage and activation of procaspase-9 [9]. However, Akt inhibits processing and activation of procaspase-9 *via* Akt-mediated phosphorylation of Ser196-procaspase-9 [10]. Thus, Akt signaling inhibits the caspase cascade at caspase-9 and is essential for the survival of KSHV-infected PEL cells.

The fullerene C_{60}, originally named buckminsterfullerene C_{60}, is a unique spherical carbon molecule [11]. Since fullerene is poorly soluble in aqueous media, many water-soluble fullerene derivatives have been developed by incorporation of hydrophilic groups into the C_{60} core. Interestingly, addition of hydrophilic groups confers upon fullerene biological activities and may facilitate its use in biomedical applications [12] such as gene and drug delivery [13], DNA photocleaving [14], extinction of reactive oxygen species (ROS) [15], generation of ROS [16], and anti-viral activity by inhibiting viral enzymes: HIV-1 protease [17], HIV reverse transcriptase [18], hepatitis C virus RNA polymerase [18] and influenza virus endonuclease [19].

Regarding the pharmacological properties of fullerenes, water-soluble fullerene derivatives could be novel compounds used with molecular target drugs for the treatment of PEL. The anti-cancer effect of water-soluble fullerenes against PEL remains unknown; therefore, we investigated whether seven water-soluble fullerene derivatives could kill PEL cells. In this study, we screened the seven fullerene derivatives (Supplemental Fig. S1) developed by Mashino et al. [15,16,18,19].

2. Materials and methods

2.1. Agents and preparation of fullerene derivatives

Akt inhibitor (1L6-hydroxymethyl-chiro-inositol-2-[R]-2-O-methyl-3-O-octadecyl-sn-glycerocarbonate), MEK inhibitor (U0126) and geldanamycin (GA) were purchased from Merck (Whitehouse Station, NJ, USA). Fullerene derivatives were synthesized and purified according to methods reported previously with small modifications [15,16,18,19]. All of the fullerene derivatives were dissolved in DMSO to 10 mM as stock solutions.

2.2. Cell lines and cell viability assay

PEL cells and KSHV-negative B-lymphoma cells were maintained in RPMI 1640 with 10% FCS. Cells were seeded in 96-well plates at 1×10^4/well in 100 μL of medium with or without a fullerene derivative at various concentrations and incubated for 24 h. Cell viability was estimated using a Cell Counting Kit-8 (Dojindo, Kumamoto, Japan) [20]. The optical density at 450 nm of each sample was measured using a microplate spectrophotometer (Tecan M200; Tecan, Kanagawa, Japan) and expressed as a percentage of the value of untreated cells (defined as 1.0).

2.3. Western blot analysis and antibodies

Western blot analysis and immunofluorescence (IF) were performed as described previously [21]. The primary antibodies, anti-Thr308phospho-Akt (558316), -Thr202/Tyr204phospho-Erk1/2 (612359), -Erk2 (610104) and -IκBα (610691), were

purchased from BD Biosciences (Franklin Lakes, NJ, USA). Anti-Ser473phospho-Akt (#9271), -Akt (#9272), -caspase-3 (#9662), -caspase-8 (#9746) and -caspase-9 (#9502) were purchased from Cell Signaling Technology (Beverly, MA, USA). Anti-β-Actin (sc-69879), -p53 (sc-126) and -Ser196phospho-caspase-9 (sc-11755) were purchased from Santa Cruz Biotechnology, Inc. (Santa Cruz, CA, USA).

2.4. Microscopy

For differential interference contrast (DIC) microscopy, cells were fixed in 4% p-formaldehyde for 30 min and incubated with Hoechst 33342 for 10 min. DIC images were obtained using an inverted microscope (Olympus IX-71; Olympus, Tokyo, Japan). For IF images, cells treated with derivative-2 were fixed with 4% p-formaldehyde and were subsequently fixed with cold methanol. Fixed cells were incubated with an anti-Ser196phospho-procaspase-9 antibody and then incubated with an Alexa594-conjugated donkey anti-rabbit IgG (Invitrogen, Carlsbad, CA, USA). Fluorescence images were obtained using an inverted confocal microscopy system (Nikon A1R+; Nikon, Tokyo, Japan).

2.5. Caspase assay

Cells (4×10^5) were incubated with 25 μM derivative-2 for 12 h and the activities of caspase-3/7, -8 and -9 in cell lysates were measured using the Caspase-Glo assay kit according to the manufacturer's protocols (Promega, Madison, WI, USA) [20]. Luminescence was measured using a luminescence microplate leader (Tecan M200). The caspase activities of untreated cells were defined as 1.0 relative light unit.

2.6. Quantification of KSHV virions

KSHV virions in medium were quantified as previously described [22]. BCBL1 cells (2×10^5) were treated with 1.5 mM n-butyrate and 25 μM derivative-2 for 24 h and then the culture media were collected. To obtain only enveloped and encapsulated viral genomes, 300 μL of media were incubated with 4 units of DNase-I for 30 min. Viral DNA was purified and extracted from 200 μL of DNase-I-treated media. To quantify viral DNA, SYBR green real-time PCR was performed using specific primers amplifying the KSHV ORF50/RTA gene (sense: 5′-TTCGTCGGCCTCTCGGAC-GAACTGA-3′, antisense: 5′-ATAATCCGAATGCACACA TCT TCCACCA C-3′).

3. Results and discussion

3.1. The cytotoxic effects of fullerene derivatives on PEL cells

First, we evaluated the cytotoxic effect of the following seven water-soluble fullerene derivatives: malonic acid (derivative-1) [15], pyrrolidinium (derivative-2) [16,18,19], proline (derivative-3–6) [18] and piperazine (derivative-7) [18] type on PEL cells (Fig. 1A–G). KSHV-infected B-lymphoma PEL cell lines (HBL6, BC2, BC3, and BCBL1) and KSHV-uninfected B-lymphoma cell lines (DG75 and Ramos) were cultured in the presence (or absence) of fullerene derivative for 24 h and viabilities were assessed using a Cell Counting Kit-8. The pyrrolidinium fullerene (derivative-2), 1,1,1′,1′-tetramethyl [60]fullerenodipyrrolidinium diiodide (also designated C_{60}-bis (N,N-dimethylpyrrolidinium iodide)), decreased the viability of PEL cells compared to KSHV-uninfected cells (Fig. 1B). Only derivative-2 prevented the proliferation of PEL cells and the anionic, proline and amino acid fullerene derivatives did not affect cell proliferation of PEL and KSHV-uninfected cell lines.
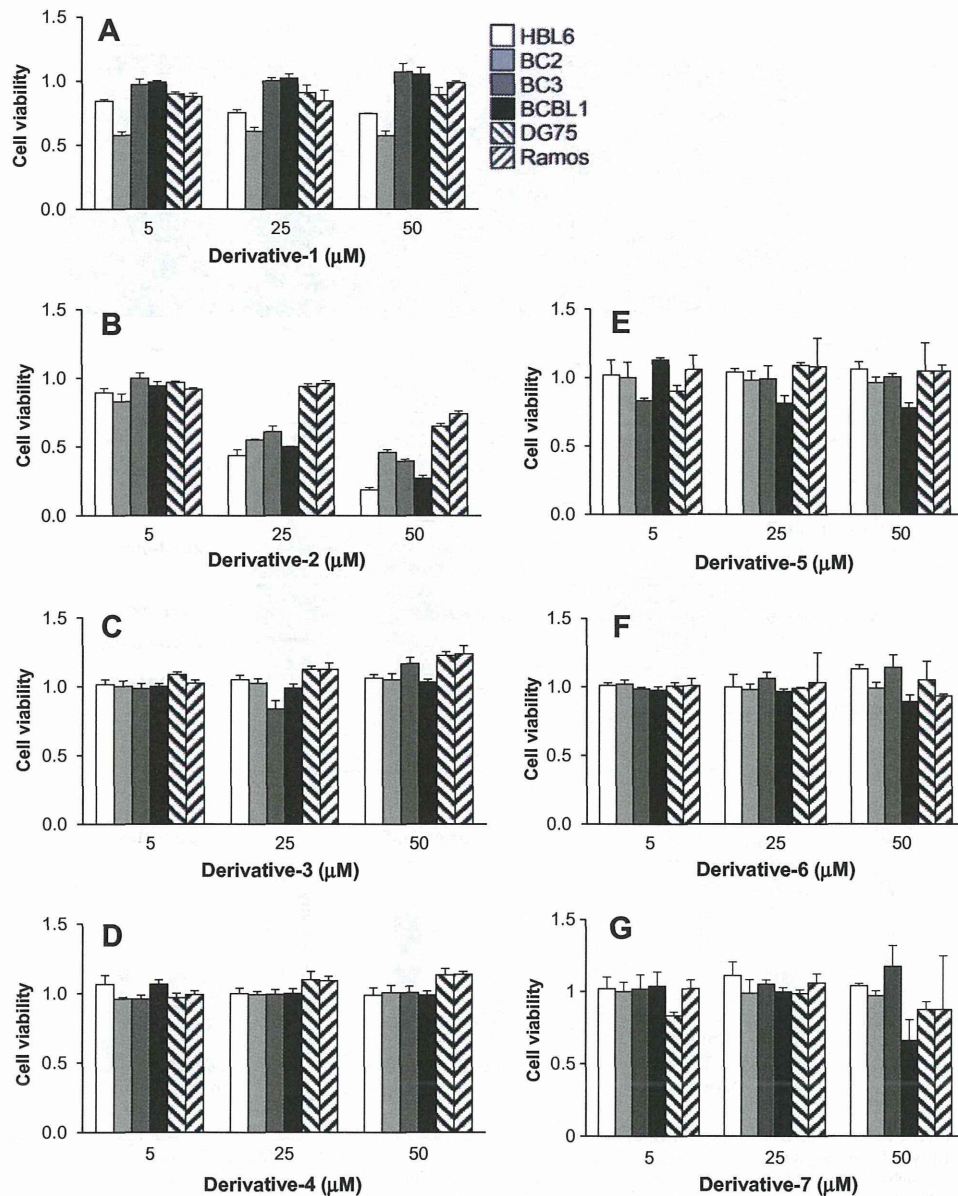
Fig. 1. The cytotoxic effects of fullerene derivatives on PEL and KSHV-uninfected lymphoma cells. KSHV[+] and EBV^{+} PEL cells (HBL6 and BC2), KSHV[+] and EBV^{−} PEL cells (BC3 and BCBL1 cells) and herpes-uninfected B-lymphoma cells (Ramos and DG75 cells) were incubated for 24 h with various concentrations of the seven water-soluble fullerenes; structures are illustrated in Supplemental Fig. 1. Fullerene derivatives evaluated for cell viability were classified into malonic acid type (derivative-1; Fig. 1A), pyrrolidinium type (derivative-2; Fig. 1B), proline type (derivative-3–6; Fig. 1C–F) or piperazine type (derivative-7; Fig. 1G). The cell-viability values of the respective untreated cells were defined as 1.0. Standard deviations were determined by analyzing the data from three independent experiments and are indicated by the error bars.

The cytotoxic effects of derivative-2 on B-lymphoma cells are summarized in Table 1. The derivative-2 was active against HBL6 and BCBL1 cells with the CC_{50} values of 18.6 and 25.0 μM, respectively, while DG75 and Ramos cells were insensitive to derivative-2 ($CC_{50} > 50$ μM). The CC_{50} values of other fullerene derivatives are

over 50.0 μM. Since derivative-2 showed strong antiproliferative activities against PEL, we focused on the cytotoxic effects of derivative-2 and analyzed the underlying molecular machinery.

3.2. Derivative-2 induces apoptosis of PEL cells by activating caspase-9 via cleavage of procaspase-9

Next we assessed the effects of derivative-2 on PEL cell morphology. Interestingly, treatment with derivative-2 induced cell–cell clumping of BC3 cells (Fig. 2A). The derivative-2 treatment also induced clumps of DG75 cells; however, the DG75 clumps were smaller than those of BC3 cells (data not shown). Because derivative-2 selectively decreased the viability of PEL cells, we investigated whether its cytotoxic effects were due to apoptosis. We
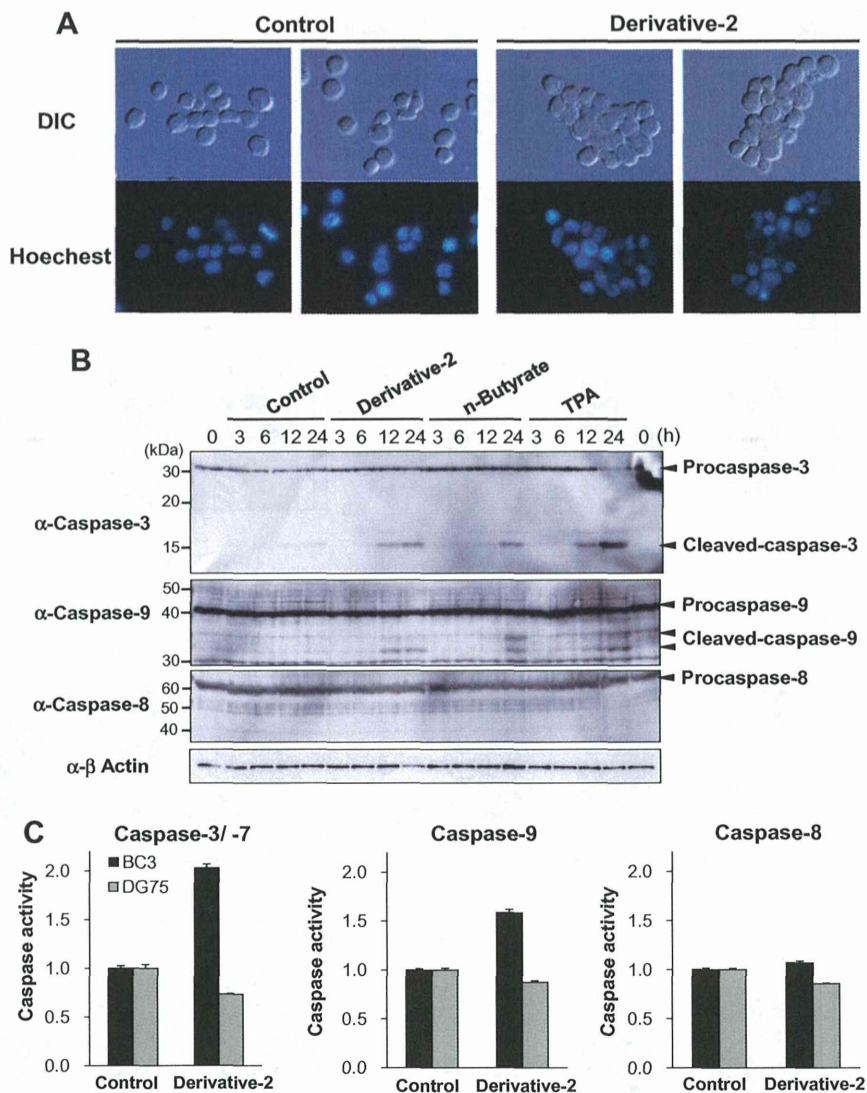
Table 1
Cytotoxic effects of pyrrolidinium fullerene (derivative-2) on B-lymphoma cells.

	HBL6	BC2	BC3	BCBL1	DG75	Ramos
CC_{50} (μM)	18.6	38.9	37.8	25.0	>50	>50

CC_{50}, cytotoxic concentration of pyrrolidinium fullerene that reduces cell viability by 50%.

Fig. 2. The pyrrolidinium-type fullerene derivative (derivative-2) induces activation of caspase-9 in PEL cells. (A) Differential interference contrast (DIC) images of cells treated with pyrrolidinium-type fullerene (derivative-2). BC3 cells were cultured with 25 μM of derivative-2 or DMSO for 6 h and then incubated with Hoechst 33342 to stain nuclear DNA. DIC images of each cell were obtained using an inverted microscope. (B) Immunoblotting using antibodies against caspase-3, -8 and -9. BC3 cells were cultured with control vehicle (DMSO), 25 μM derivative-2, or 1.5 mM n-butyrate (or 20 ng/mL TPA) as the positive control for induction of apoptosis. (C) Changes in the proteolytic activities of caspase-3/7, -9 and -8 in PEL cells treated with derivative-2. BC3 cells were incubated with 25 μM derivative-2 for 12 h. The caspase activity, represented by relative light units, in untreated cells was defined as 1.0.

monitored the cleavage (i.e., activation) of caspase-3, -9 and -8 in BC3 cells pretreated with derivative-2 and positive controls (n-butyrate and TPA). The active large fragment (17 kDa) cleaved from procaspase-3 was detected in BC3 cells treated with derivative-2 (Fig. 2B). Levels of the active caspase-9 subunits (35 and 37 kDa), which are produced by proteolytic processing of procaspase-9 (42 kDa), were also increased in BC3 cells treated with derivative-2. In contrast, cleavage of caspase-8 was not detected. To obtain further evidence of apoptosis induction, we monitored the peptidase activity of caspase-3/7, -9 and -8 in BC3 cells pretreated with derivative-2 using a colorimetric assay (Fig. 2C). Compared to treatment with the DMSO control, treatment with derivative-2 increased caspase-3/7 and -9 activities in BC3 but not DG75 cells.

These results indicate that derivative-2 suppressed the growth of PEL cells by triggering apoptosis, mediated by the activation of procaspase-9 via proteolytic cleavage resulting in activation of executioner caspases such as caspases-3 and -7. Derivative-2

additionally induced cell–cell clumping; however, the mechanism of fullerene-dependent clumping remains unclear. The association between clumping and the antiproliferative effects on PEL cells should be investigated in future studies.

3.3. Derivative-2 suppresses Akt signaling and phosphorylation of procaspase-9

Akt [7], Erk [7] and NF-κB [20,23] signaling are activated in PEL and are necessary for the survival and proliferation of PEL cells. Therefore, we investigated whether derivative-2 influenced Akt, Erk and NF-κB signaling. When BC3 cells were treated with derivative-2 for 6 and 12 h, the extent of phosphorylation of Ser473 in Akt (p-Akt) and phosphorylation of Thr202/Tyr204 in Erk1/2 (p-Erk1/2) were decreased compared to treatment with the control vehicle, whereas Ser308 phosphorylation in Akt was unchanged (Fig. 3A and B). The levels of p53 and IκBα protein (an inhibitor
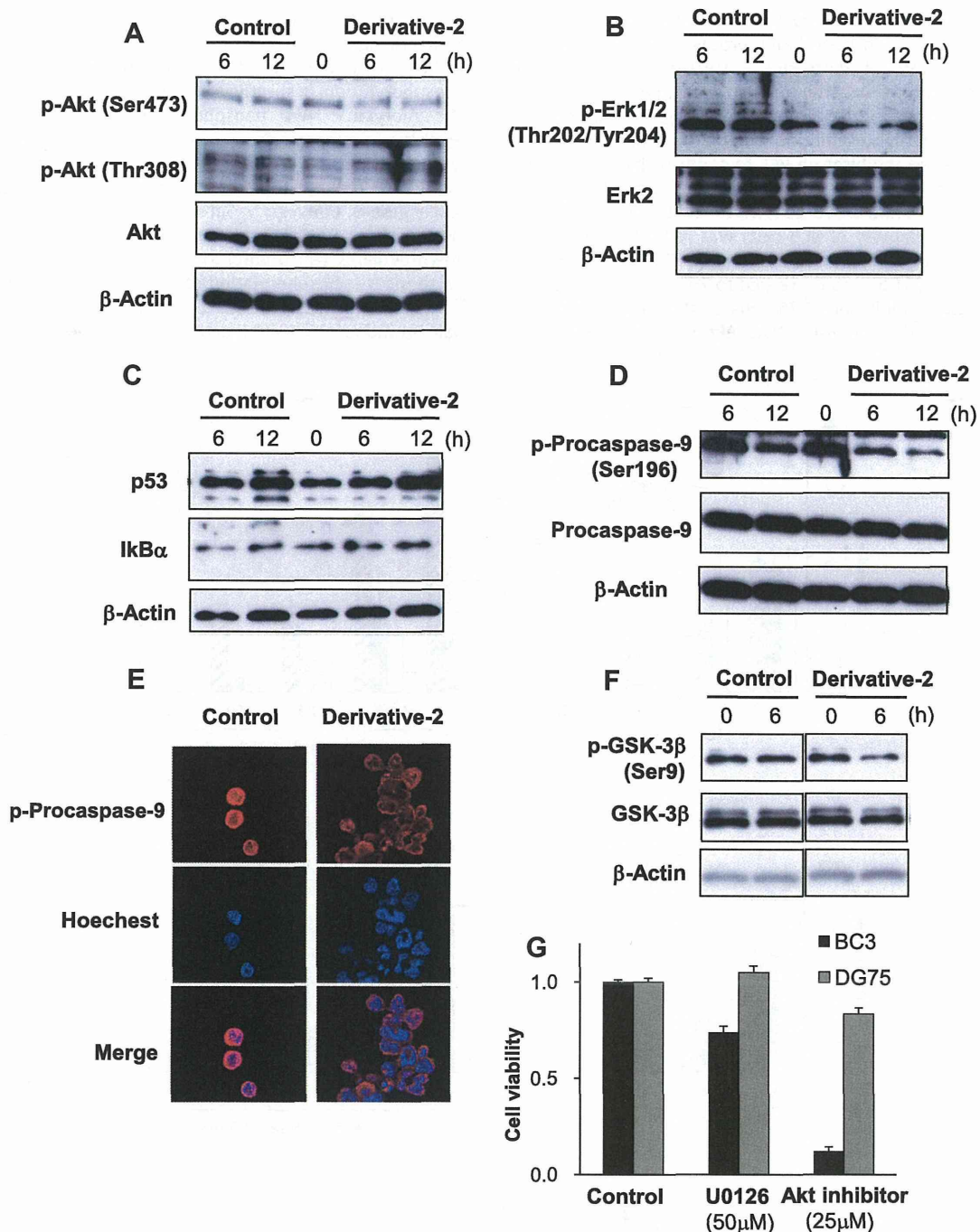
Fig. 3. Derivative-2 suppresses phosphorylation of Akt, Erk and procaspase-9 in PEL cells. (A and B) Suppression of Ser473 phosphorylation at Akt and Thr202/Tyr204 at Erk1/2 in PEL cells caused by derivative-2. BC3 cells were cultured with 25 μM derivative-2 or control vehicle (DMSO) for 0, 6, or 12 h and then harvested. To elucidate Akt and Erk activities, whole-cell lysates were analyzed by Western blotting with anti-Ser473-phospho-Akt, anti-Thr308-phospho-Akt and anti-Thr202/Tyr204-phospho-Erk1/2 antibodies. (C and D) Derivative-2 effects on the amount of p53, IkBα and Ser196-phosphorylated procaspase-9 in BC3 cells. Cells were cultured with 25 μM derivative-2 and cell lysates were subjected to immunoblotting with anti-p53, -IkBα and -Ser196-phosho-procaspase-9 antibodies. (E) Immunofluorescence (IF) assay of Ser196 procaspase-9 phosphorylation in BC3 cells treated with derivative-2. BC3 cells treated with 25 μM derivative-2 for 12 h were stained with anti-Ser196-phosho-procaspase-9 and then incubated with Alexa594-conjugated anti-rabbit IgG and Hoechest33342 (to stain the nucleus). (F) Suppression of GSK-3β Ser9 phosphorylation in BC3 cells caused by derivative-2. BC3 cells were cultured with 25 μM derivative-2 for 6 h and cell lysates were subjected to blotting with anti-Ser9-phospho-GSK-3β antibody. (G) The cytotoxic effects of a MEK inhibitor (U0126) or an Akt inhibitor on PEL cells. BC3 and KSHV-uninfected Ramos cells were incubated with U0126 or Akt inhibitor for 24 h and then assessed for viability.

of NF-κB) were unaffected by derivative-2 (Fig. 3C). Ser473-phosphorylated Akt (activated Akt) phosphorylates its substrates, such as procaspase-9 and GSK-3β [8–10]. Because derivative-2 reduced Ser473-phosphorylated Akt, we examined whether derivative-2

affected the phosphorylation of procaspase-9 and GSK-3β. When BC3 cells were treated with derivative-2 for 6 and 12 h, Ser196 phosphorylation of procaspase-9 was decreased as compared with the control vehicle (Fig. 3D). We confirmed the suppression of

procaspase-9 phosphorylation by derivative-2 using an IF assay. The level of Ser196-phosphorylated procaspase-9 was reduced 12 h after the start of derivative-2 treatment in BC3 cells (Fig. 3E). Furthermore, treatment with derivative-2 resulted in decreased Ser9 phosphorylation in GSK-3β (Fig. 3F). In addition, we measured the cytotoxic effects of a U0126, a MEK (Erk kinases) inhibitor and an Akt inhibitor on PEL to confirm that Erk and Akt signaling contribute to the growth and survival of PEL cells (Fig. 3G). When BC3 and DG75 cells were treated with U0126 or Akt inhibitor, the viability of BC3 cells was reduced significantly by the Akt inhibitor compared to DG75 cells. The viability of BC3 cells treated with U0126 was decreased to 75% of the vehicle control, whereas the viability of DG75 cells treated with U0126 was unchanged. These data indicate that Akt signaling contributes

significantly to the survival and proliferation of PEL compared with MEK–Erk signaling.

PDK1-PI3K and mTORC2 induce Ser308-Akt and Ser473-Akt phosphorylation, respectively, causing Akt activation [8]. Ser473-phosphorylated Akt phosphorylates Ser196 in procaspase-9, resulting in suppression of activation of procaspase-9 by proteolytic cleavage [9,10]. Thus, Akt contributes to suppression of the cascade of caspase-9-mediated apoptosis by phosphorylation of procaspase-9. Conversely, Ser473-phosphorylated Akt phosphorylates Ser9 at GSK-3β, causing GSK-3β inactivation [8]. GSK-3β downregulates cell proliferation, glycogen synthesis and protein synthesis by phosphorylation of cyclin D1, glycogen synthase and eIF2B, respectively. Akt-mediated phosphorylation of Ser9 at GSK-3β induces GSK-3β inactivation by inhibiting the active site
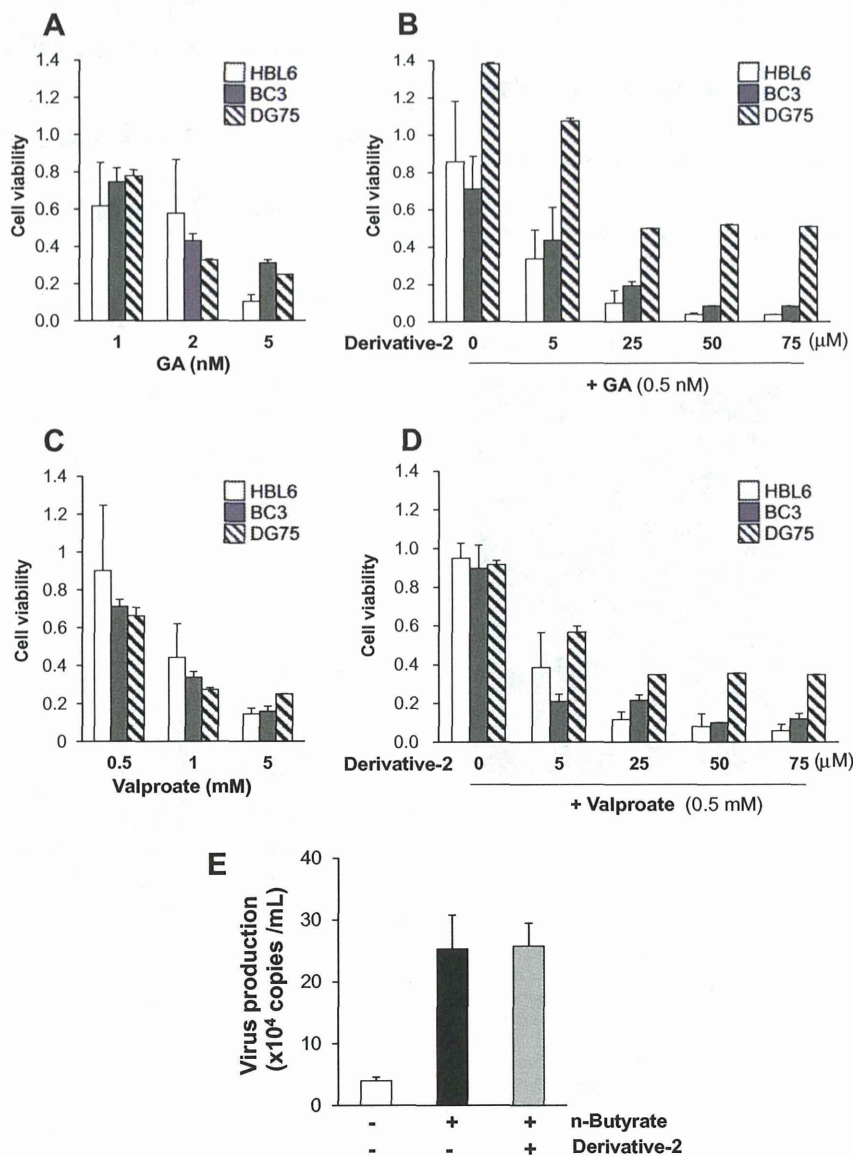

Fig. 4. Facilitation of derivative-2 cytotoxic activities with a low concentration of geldanamycin (GA) or valproate against PEL cells. (A and B) The cytotoxic effect of GA alone or in combination with derivative-2 on PEL cells. PEL cells (HBL6 and BC3), or KSHV-uninfected DG75 cells were cultured with 1, 2, or 5 nM GA (A) or a combination of 0.5 nM GA and 0, 5, 25, 50, or 75 µM derivative-2 (B) for 24 h and cell viability was measured. The viability of untreated cells was defined as 1.0. (C and D) The cytotoxic effect of valproate alone or in combination with derivative-2 on PEL cells. HBL6, BC3 or DG75 cells were treated with 0.5, 1 or 5 mM valproate or a combination of 0.5 mM valproate and derivative-2 and cultured for 24 h. (E) Derivative-2 effects on KSHV replication in BCBL1 cells. BCBL1 cells were cultured for 24 h with or without 25 µM derivative-2 in the presence of 1.5 mM n-butyrate. Culture medium containing virus particles was harvested and KSHV genome copy numbers were quantified by real-time PCR.

availability of GSK-3β [8]; thus, Akt promotes cell proliferation and glycogen synthesis *via* GSK-3β-phosphorylation. We showed that derivative-2 induced activation of procaspase-9 (Fig. 2B and C) and reduced Akt phosphorylation at Ser473 and procaspase-9 at Ser196 in PEL cells. In addition, derivative-2 resulted in decreased Ser9 phosphorylation in GSK-3β. Collectively, these data suggest that derivative-2 induced activation of caspase-9 and inhibition of cell proliferation in PEL cells by suppressing Akt, which plays an important role in inactivation of caspase-9 and GSK-3β.

Because derivative-2 suppressed Erk1/2 phosphorylation (Fig. 3B), we examined the effects of derivative-2 on other MAPKs; however, unlike Erk1/2, derivative-2 did not change the phosphorylation of p38 MAPK and JNK (data not shown). Akt [4,7] and Erk [4,7,22,24] signaling are activated in PEL to maintain the malignant phenotype and to ensure PEL cell survival. In particular, KSHV activates Raf-MEK-Erk signaling, allowing the establishment of a KSHV infection [24] and survival of KSHV-infected cells [7]. We found that derivative-2 suppressed the phosphorylation of Erk1/2 as well as Akt; thus inhibition of Erk signaling also contributed to PEL cell apoptosis.

In this report, four groups of water-soluble fullerene derivatives were evaluated in terms of their effect on cell proliferation. Our data demonstrated that only the pyrrolidinium-type fullerene (derivative-2), which induces apoptosis of HL-60 cells by ROS generation [16], decreased the viability of KSHV-infected PEL cells but not KSHV-uninfected B-lymphoma cells (Fig. 1B). We examined whether derivative-2 induced the mitochondrial abnormalities caused by ROS; release of cytochrome c from mitochondria was observed in both PEL cells and KSHV-uninfected B-lymphoma cells (data not shown), indicating that derivative-2 induces apoptosis only in PEL cells by an ROS generation-independent mechanism, which is closely related to Akt suppression and caspase-9 activation.

3.4. Derivative-2 in combination with geldanamycin (GA) or valproate enhances the cytotoxic effects on PEL cells

Generally, combined therapies for treatment of cancer, including lymphoma, are more effective than monotherapies. We previously found that the HSP90 inhibitor, geldanamycin (GA), induced apoptosis in PEL [23]. Furthermore, valproate (sodium valproate) reportedly also induces apoptosis in PEL cells, accompanied by KSHV reactivation [25]. Therefore, we investigated whether derivative-2 treatment in combination with low concentrations of GA or valproate enhanced the cytotoxic effects of derivative-2 on PEL cells. When PEL (HBL6 and BC3 cells) were treated with GA alone (Fig. 4A) or valproate alone (Fig. 4C) for 24 h, treatment with 1 nM GA and 0.5 nM valproate slightly affected PEL cell proliferation. Next, PEL cells were treated with a combination of various concentrations of derivative-2 and 0.5 nM GA (Fig. 4B) or 0.5 nM valproate (Fig. 4D). The combination treatment with GA or valproate resulted in significantly decreased cell viability of HBL6 and BC3 cells compared with derivative-2 alone (Fig. 1B). As shown in Fig. 1B, 25 μM derivative-2 alone decreased cell viability to approximately 50% of the vehicle control, whereas the viability of HBL6 and BC3 cells treated with the combination of 25 μM derivative-2 with 0.5 nM GA (or 0.5 mM valproate) decreased to less than 20%. Thus, the combination of derivative-2 with a low concentration of GA or valproate enhanced the suppression of PEL cell proliferation in a synergistic manner. Combination treatment with such drugs is a novel chemotherapeutic strategy for PEL. Finally, we examined the effect of derivative-2 on lytic replication in PEL cells. Treatment with 1.5 mM *n*-butyrate induced viral replication in KSHV-infected BCBL1 cells, and co-treatment with 1.5 mM *n*-butyrate and 25 μM derivative-2 did not affect KSHV lytic replication in BCBL1 cells (Fig. 4E). These data show that derivative-2 induces apoptosis in PEL cells without production of

progeny virus. Thus, the present study provided a rationale indicating derivative-2 as a potential molecular candidate agent for PEL treatment without *de novo* KSHV production and infection.

Acknowledgments

Appendix A. Supplementary data

Supplementary data associated with this article can be found, in the online version, at http://dx.doi.org/10.1016/j.bbrc.2014.07.068.

References

[1] J.J. Russo, R.A. Bohenzky, M.C. Chien, J. Chen, M. Yan, D. Maddalena, J.P. Parry, D. Peruzzi, I.S. Edelman, Y. Chang, P.S. Moore, Nucleotide sequence of the Kaposi sarcoma-associated herpesvirus (HHV8), Proc. Natl. Acad. Sci. U.S.A. 93 (1996) 14862–14867.

[2] R.G. Nador, E. Cesarman, A. Chadburn, D.B. Dawson, M.Q. Ansari, J. Said, D.M. Knowles, Primary effusion lymphoma: a distinct clinicopathologic entity associated with the Kaposi's sarcoma-associated herpes virus, Blood 88 (1996) 645–656.

[3] Y. Chang, E. Cesarman, M.S. Pessin, F. Lee, J. Culpepper, D.M. Knowles, P.S. Moore, Identification of herpesvirus-like DNA sequences in AIDS-associated Kaposis sarcoma, Science 266 (1994) 1865–1869.

[4] A. Järviluoma, P.M. Ojala, Cell signaling pathways engaged by KSHV, Biochim. Biophys. Acta 1766 (2006) 140–158.

[5] M. Fujimuro, F.Y. Wu, C. apRhys, H. Kajumbula, D.B. Young, G.S. Hayward, S.D. Hayward, A novel viral mechanism for dysregulation of β-catenin in Kaposis sarcoma-associated herpesvirus latency, Nat. Med. 9 (2003) 300–306.

[6] A. Ashizawa, C. Higashi, K. Masuda, R. Ohga, T. Taira, M. Fujimuro, The ubiquitin system and Kaposi's sarcoma-associated herpesvirus, Front. Microbiol. 3 (2012) 66.

[7] M.J. Smit, D. Verzijl, P. Casarosa, M. Navis, H. Timmerman, R. Leurs, Kaposi's sarcoma-associated herpesvirus-encoded G protein-coupled receptor ORF74 constitutively activates p44/p42 MAPK and Akt via G(i) and phospholipase C-dependent signaling pathways, J. Virol. 76 (2002) 1744–1752.

[8] C. Fumarola, M.A. Bonelli, P.G. Petronini, R.R. Alfieri, Targeting PI3K/AKT/mTOR pathway in non small cell lung cancer, Biochem. Pharmacol. 90 (2014) 197–207.

[9] S.B. Bratton, G.S. Salvesen, Regulation of the Apaf-1–caspase-9 apoptosome, J. Cell Sci. 123 (2010) 3209–3214.

[10] M.H. Cardone, N. Roy, H.R. Stennicke, G.S. Salvasen, T.F. Franke, E. Stanbridge, S. Frisch, J.C. Reed, Regulation of cell death protease caspase-9 by phosphorylation, Science 282 (1998) 1318–1321.

[11] H.W. Kroto, J.R. Heath, S.C. O'Brien, R.F. Curl, R.E. Smalley, C60: buckminsterfullerene, Nature 318 (1985) 162–163.

[12] S. Nakamura, T. Mashino, Water-soluble fullerene derivatives for drug discovery, J. Nippon Med. Sch. 79 (2012) 248–254.

[13] H. Isobe, W. Nakanishi, N. Tomita, S. Jinno, H. Okayama, E. Nakamura, Nonviral gene delivery by tetraamino fullerene, Mol. Pharm. 3 (2006) 124–134.

[14] H. Tokuyama, S. Yamago, E. Nakamura, T. Shiraki, Y. Sugiura, Photoinduced biochemical activity of fullerene carboxylic acid, J. Am. Chem. Soc. 115 (1993) 7918–7919.

[15] K. Okuda, T. Mashino, M. Hirobe, Superoxide radical quenching and cytochrome c peroxidase-like activity of C_{60}-dimalonic acid, $C_{64}(COOH)_4$, Bioorg. Med. Chem. Lett. 6 (1996) 539–542.

[16] C. Nishizawa, N. Hashimoto, S. Yokoo, M. Funakoshi-Tago, T. Kasahara, K. Takahashi, S. Nakamura, T. Mashino, Pyrrolidinium-type fullerene derivative-induced apoptosis by the generation of reactive oxygen species in HL-60 cells, Free Radic. Res. 43 (2009) 1240–1247.

[17] S.H. Friedman, D.L. DeCamp, R.P. Sijbesma, G. Srdanov, F. Wudl, G.L. Kenyon, Inhibition of the HIV-1 protease by fullerene derivatives: model building studies and experimental verification, J. Am. Chem. Soc. 115 (1993) 6506–6509.

[18] T. Mashino, K. Shimotohno, N. Ikegami, D. Nishikawa, K. Okuda, K. Takahashi, S. Nakamura, M. Mochizuki, Human immunodeficiency virus-reverse transcriptase inhibition and hepatitis C virus RNA-dependent RNA polymerase inhibition activities of fullerene derivative, Bioorg. Med. Chem. Lett. 15 (2005) 1107–1109.

[19] M. Shoji, E. Takahashi, D. Hatakeyama, Y. Iwai, Y. Morita, R. Shirayama, N. Echigo, H. Kido, S. Nakamura, T. Mashino, T. Okutani, T. Kuzuhara, Anti-influenza activity of c60 fullerene derivatives, PLoS One 8 (2013) e66337.

[20] C. Saji, C. Higashi, Y. Niinaka, K. Yamada, K. Noguchi, M. Fujimuro, Proteasome inhibitors induce apoptosis and reduce viral replication in primary effusion lymphoma cells, Biochem. Biophys. Res. Commun. 415 (2011) 573–578.

[21] M. Fujimuro, J. Liu, J. Zhu, H. Yokosawa, S.D. Hayward, Regulation of the interaction between glycogen synthase kinase 3 and the Kaposi's sarcoma-associated herpesvirus latency-associated nuclear antigen, J. Virol. 79 (2005) 10429–10441.

[22] K. Wakao, T. Watanabe, T. Takadama, S. Ui, Z. Shigemi, H. Kagawa, C. Higashi, R. Ohga, T. Taira, M. Fujimuro, Sangivamycin induces apoptosis by suppressing Erk signaling in primary effusion lymphoma cells, Biochem. Biophys. Res. Commun. 444 (2014) 135–140.

[23] C. Higashi, C. Saji, K. Yamada, H. Kagawa, R. Ohga, T. Taira, M. Fujimuro, The effects of heat shock protein 90 inhibitors on apoptosis and viral replication in primary effusion lymphoma cells, Biol. Pharm. Bull. 35 (2012) 725–730.

[24] P.P. Naranatt, S.M. Akula, C.A. Zien, H.H. Krishnan, B. Chandran, Kaposi's sarcoma-associated herpesvirus induces the phosphatidylinositol 3-kinase-PKC-zeta-MEK-ERK signaling pathway in target cells early during infection: implications for infectivity, J. Virol. 77 (2003) 1524–1539.

[25] C.M. Klass, L.T. Krug, V.P. Pozharskaya, M.K. Offermann, The targeting of primary effusion lymphoma cells for apoptosis by inducing lytic replication of human herpesvirus 8 while blocking virus production, Blood 105 (2005) 4028–4034.